Reversible shear thickening at low shear rates of electrorheological fluids under electric fields

Yu Tian, Minliang Zhang, Jile Jiang, Noshir Pesika, Hongbo Zeng, Jacob Israelachvili, Yonggang Meng, and Shizhu Wen

Phys. Rev. E **83**, 011401 — Published 5 January 2011

DOI: 10.1103/PhysRevE.83.011401

Reversible shear thickening at low shear rates of electrorheological fluids under electric fields

Yu Tian,[1]* Minliang Zhang,[1] Jile Jiang,[1] Noshir Pesika,[2] Hongbo Zeng,[3] Jacob Israelachvili,[4] Yonggang Meng,[1] Shizhu Wen[1]

1. State Key Laboratory of Tribology, Department of Precision Instruments, Tsinghua University, Beijing 100084, P. R. China
2. Department of Chemical and Biomolecular Engineering, Tulane University, LA 70118, USA
3. Department of Chemical and Materials Engineering, University of Alberta, AB, T6G 2V4, Canada
4. Department of Chemical Engineering, Materials Research Laboratory, University of California, Santa Barbara, California 93106, USA

Abstract

By shearing electrorheological (ER) fluids between two concentric cylinders, we show a reversible shear thickening of ER fluids above a low critical shear rate (<1 s^{-1}) and a high critical electric field strength (>100 V/mm), which could be characterized by a critical apparent viscosity. Shear thickening and electrostatic particle interaction-induced inter-particle friction forces is considered to play an important role in the origin of lateral shear resistance of ER fluids, while the applied electric field controls the extent of shear thickening. The electric field-controlled reversible shear thickening has implications for high-performance ER/magnetorheological (MR) fluid design, clutch fluids with high friction forces triggered by applying local electric field, other field-responsive materials and intelligent systems.

PACS: 82.70.Dd; 61.30.Gd; 81.05.Rm

***Correspondence to:** tianyu@mail.tsinghua.edu.cn

1. Introduction

Colloidal suspensions have attracted much interest because of their wide range of applications, such as in decorative or protective paints, laser printer ink, and advanced pharmaceutical drug delivery [1-3]. Shear thickening is a phenomenon of significant viscosity change of colloidal suspensions and has recently been exploited to fabricate advanced flexible liquid armors [4-6]. ER and MR fluids are electric and magnetic field responsive colloidal suspensions [7-15], the rheological properties of which can be abruptly altered from a Newtonian fluid with $\tau = \eta_0 \dot{\gamma}$ into a Bingham fluid with $\tau = \tau_E + \eta_0 \dot{\gamma}$, where τ is the shear stress, η_0 is the viscosity of the suspension under zero electric field, $\dot{\gamma}$ is the shear rate, and τ_E is the shear yield stress. Since the invention of ER and MR fluids by Winslow [7] and Robinnow [11], shear yield stress has been represented by the electrostatic/magnetic attractive strength between ER/MR particles with various polarization models [7-14].

A general ER fluid has a shear yield stress of several kPa and requires a local electric field between particles in the order of 10 kV/mm [7-9,15]. However, a recently developed "giant ER fluid" has shown a yield stress over 100 kPa [10,16] and was claimed to have a different mechanism from the traditional ER effect since it requires a rather high local electric field between particles in the order of 100 kV/mm. This local electric field is even higher than the breakdown electric field of most insulating liquids. The magnitudes of the local electric field and the attractive electrostatic field strength between ER particles with nanometer gap distances have not been experimentally quantified due to experimental difficulties.

Experimental and theoretical studies have only been done to explore the formation of particle chains and columnar structures in the static equilibrium state [17-19], as well as the shear-induced striped/lamellar structures, both in ER and MR fluids [20-23]. Fig. 1a shows a schematic of ER particles under conditions of zero electric field (randomly distributed), high electric fields (columns along the field direction), and high electric fields in addition to shearing (stripes and lamellar structures along the shear direction). However, the relationships between the rheological properties of ER/MR fluids and their chain structure under an electric/magnetic field have not been well understood. Most available models predict the shear strength of ER/MR fluids by considering attractive electrostatic/magnetic forces due to the dipole-dipole or multipole interactions between particles as shown in Fig. 1b, where the particle interaction potential $U(r, \theta)$ is related to the dipolar strength μ, the distance between particle centers r, and the angle θ of particle center line to field direction, without including the structural evolution of ER/MR fluids during shearing [8,9,13,14].

In this study, ER fluids were sheared between two concentric cylinders on a commercial rheometer (Physica MCR 301). A reversible shear thickening of ER fluids above a low critical shear rate (<1 s^{-1}) and a high critical electric field strength (>100 V/mm) has been found. The electric field controlled shear thickening was verified with various experimental test modes or methods, ER fluids with different particle types, particles volume fractions, insulating medium viscosities, and characterized by a modified Mason number or more generally, a critical bulk viscosity of the ER fluid under electric fields. When ER fluids are shear thickened or jammed, where direct mechanical contact between particles may occur,

how the mechanical contact load L along with the electrostatic attractive force $F(r, \theta)$ contribute to the lateral shear resistance has not been discussed yet. A possible mechanism is suggested in this study as sketched in Fig. 1c, both L and $F(r, \theta)$ act as compressive loads acted on particles to produce a friction force through a friction coefficient factor f when particles are forced to have a relative motion. The friction force is responsible for the lateral shear resistance of the bulk ER fluid. The applied electric field controls the extent of shear thickening.

2. Materials and Methods

In this study, the ER fluid consisted of NaY zeolite particles [15] (Qilu Petro. Corp., Shandong, China) with density of 1.85 g/cm^3, average diameter of 1 μm, and silicone oil (Beijing Chem. Corp., China) with viscosity of 10 mPa.s at room temperature 20 °C, density of 0.93 g/cm^3, and dielectric constant of 2.56. The zeolite particles were washed with de-ionized water several times and then dried in a microwave oven. A mixture of 1:9 glycerin/ethanol was then combined with the dry zeolite particle to obtain a weight ratio of 1% glycerin to zeolite particles, which results in a thin coating of glycerin on the zeolite particles with a thickness of less than 6 nm to get a stronger ER effect [8,10-11,15,16]. Silicone oil was used as received. Zeolite particles were mixed with silicone oil in a four-roll miller to obtain a uniform ER suspension. The shear tests were done on a commercial rheometer (Physica MCR 301, Anton Paar, Germany) that have two concentric cylinders, with an inner diameter of 16.66 mm, length of 25 mm, and gap of h=0.7 mm. The electric field and the shear rate are controlled by the rheometer. In the shear rate ramp tests, the shear rate is

logarithmically ramped up from 0.01 to 50 s^{-1} in 180 s, and then subsequently logarithmically ramped down from 50 to 0.01 s^{-1} in 180 s.

3. Results and Discussion

3.1 Shear thickening of ER fluids found in shearing tests

As shown in Fig. 2a, a typical Newtonian behavior with η_0=0.06 Pa.s under zero electric field and a Bingham fluid behavior with a finite τ_E were obtained when the applied electric field is lower than 900 V/mm. When the applied field is higher than 900 V/mm, as $\dot{\gamma} \to 0$, the shear stress approaches a static yield stress τ_s (the peak value at low shear rate on the curve is taken as the static yield stress of the ER fluid in this study), which shows to be much higher than τ_E. Only when the shear rate is higher than about 10 s^{-1}, the ER fluid shows a Bingham behavior. The fitted viscosities of the ER fluid by the Bingham model are 2.2 Pa.s (715 V/mm), 3.6 Pa.s (900/mm) and 2.7 Pa.s (1430 V/mm), respectively. They change with *E* and are obviously different from the viscosity of silicone oil of 10 mPa.s and zero field viscosity of the suspension of 0.06 Pa.s. Under high fields, the viscosity would generally approach to zero and may even become negative when serious slip occurs at the ER fluid/electrode interface [11]. As the shear curves are replotted in Fig. 2b, shear stress shows an abrupt, significant, and reversible change of shear stress, occurring around a certain critical shear rate $\dot{\gamma}_c$ and above a critical electric field E_c, higher than 900 V/mm in this test. An abrupt increase of shear stress or viscosity in colloid suspensions under a constant shearing is usually referred to as shear thickening [24, 25], which is induced by arresting and pushing particles against one another. The occurrence of the abrupt and reversible increase of shear

stress observed in ER fluids can also be considered as shear thickening. The shear thickening and un-thickening happened around similar critical shear rates, showing a reversible shear thickening. And this reversibility does not refer to the shear stress change upon the applying or removal of an electric field. Figure 2b shows that no shear thickening is observed when $E <$ 900 V/mm. As E increases from 900 to 2900 V/mm, the critical shear rate $\dot{\gamma}_c$ for shear thickening increases from 0.02 to 0.2 s^{-1}, and the ratio of shear stress change, τ_H/τ_L increases from about 1.5 to 3.2 (shown in Fig. 2c, the values of τ_H and τ_L are the high shear stress and the low shear stress during shear thickening as shown in Fig. 2b. In this study, τ_H is the same as the static yield stress τ_s.). After the abrupt shear thickening, shear stress decreases with the increase of shear rate in the range of about 0.1 ~10 s^{-1}. A higher E corresponds to a more significant shear thinning. When shear rate is higher than about 10 s^{-1}, the ER fluid shows a viscous slope. On the other hand, the decrease of the shear stress when the shear rate increases can also be comprehended as a phenomenon associated to a mechanical instability of shearing non-homogeneous materials, indicating the destroying of particle structures in the shear rate range of up to 10 s^{-1}.

Prior studies have shown that a shear yield strain γ_y of about 0.3 is needed to reach the static yield stress τ_s of an ER fluid [8,14]. In Fig. 2, the shear rate is logarithmically ramped up from 0.01 to 50 s^{-1} in 180 seconds and 60 points, and subsequently ramped down. Each shear rate only lasted for 3 seconds. The shear strain at low shear rates may not exceed the shear yield strain to reach a stationary state. So the shearing time effect on the result has been experimentally studied. Shear stress with different shearing time (0.5-10 s/point) at each shear

rate shows similar shear stress amplitude, and also abruptly jumps at similar critical shear rate. Further, to confirm that the shear thickening shown in Fig. 1b is just governed by the shear rate rather than the shear strain, experiments under the same E = 2150 V/mm but different constant shear rates $\dot{\gamma}$ in the range of 0.02-0.09 s^{-1} were performed. The results are shown in Fig. 3a and 3b. When $\dot{\gamma} < \dot{\gamma}_c$, the shear stress remains low and independent of shear strain. On the other hand, when $\dot{\gamma} \geq \dot{\gamma}_c$, the shear stress is high even at a small shear strain of 0.1 (10%), which is less than the general shear yield strain of 0.3 (30%). The amplitudes of shear stress achieved at a different $\dot{\gamma}$ agree well with the shear rate ramp test. The critical shear rate $\dot{\gamma}_c$ between 0.085 and 0.09 s^{-1} is also consistent with that of 0.08-0.12 s^{-1} obtained in the shear rate ramp test. This experiment verified that the shear thickening is indeed governed by the shear rate and not the shear strain, and it also indicates that the shearing time does not affect the shear stress jump phenomenon shown in Fig. 2.

Since in this study a higher E applied on ER fluid induces a larger local electric field E_{loc} between ER particles, a larger bulk electrical current I, and a higher shear yield stress τ_E [26], the current I was simultaneously measured to represent the E_{loc} change during shearing. A typical result is shown in Fig. 3c. Accompanying the abrupt increase in shear stress during shear thickening, I decreased sharply but only slightly. This indicates a small decrease in E_{loc} between particles, which could be ascribed to the dilatancy of ER fluid that usually happens during the shear thickening or jamming of colloidal suspensions [4-5]. Dilatancy that caused less dense particle packing in an ER fluid usually corresponds to a lower E_{loc} [22]. During the reverse process (that is, decreasing the shear rate), I slightly increased, which corresponds to

the un-shear thickening process of ER fluid. This behavior is shown in Fig. 3c. It should be noted that the onset of shear thickening and un-thickening in Fig. 3b do not coincide with each other. However, they may coincide with each other as shown in Fig. 3c. But the deviation shown in Fig. 2b and 3b is more general than coinciding with each other (Fig. 3c). There are different structures in the shear rate ramp up and down processes depending on different shear history of ER fluids. However, the critical shear rate during shear rate ramp down coincides with the shear rate of the begin of an obvious shear stress increase during shear rate ramp up, as shown in Fig. 2b and 3b. It shows that the onset of shear thickening needs a certain pre-sheared particle structure. While for the onset of un-thickening of shear stress jump down, it directly switches from the thickened structure to the un-thickened structure.

As shown in Fig. 3c, the current along with the shear stress increased slowly from about 18 to 26 μA when shear rate is lower than 0.03 s^{-1}. It represents a rearrangement of particle chains under *E* and shearing. Particles are stretched to more regularly face each other to result in higher local electric field and electric current, along with a rapid shear stress increase. It can be comprehended as the traditional yielding process of ER fluid [8]. Subsequently, in the shear rate range of 0.03 to 0.1 s^{-1}, the current remains relatively stable. After shear thickening, the current decreases with the increase of shear rate, indicating a decrease of local electric field between particles. While the increase of shear stress in this region may be ascribed to the further chain aggregation. Ramping shear rate from 50 to 0.001 s^{-1}, both the current and the shear stress are different from the values during shear rate ramp up test. It can be ascribed to

the different particle structures after ER fluid experienced different shear histories.

3.2 Mechanism of Shear thickening happened in ER fluids

Shear thickening in a colloid suspension would occur when the compressive hydrodynamic force between two particles is larger than the total repulsive force between these particles [4,5,24,25]. A scaling theory takes the ratio of hydrodynamic force to the Brownian force $\tau_{cr}^{Br} = F_{hydrodynamic} / F_{Brownian}$ as an effective dimensionless critical shear stress to predict the onset of shear thickening, which agrees well with the tests of suspensions with different particle sizes and particle concentrations [5].

In research on ER effect, the Mason number [14]

$$Mn = \frac{\eta_c \dot{\gamma}}{2\varepsilon_0 \varepsilon_c \beta \mathrm{E}_0^{\,2}} \qquad (1),$$

which is the ratio of the viscous force to the attractive electrostatic force between the particles, has been used to characterize the rheological change of ER fluids. In Equation (1), η_c is the viscosity of the continuous fluid, ε_0 is the dielectric permittivity of vacuum, ε_c is the relative dielectric constant of the continuous fluid, β is the polarization ratio of particles under an external electric E_0. However, *Mn* for the results shown in Fig. 2 does not indicate a single characteristic value for shear thickening. We therefore propose a modified Mason number as

$$Mn^* = \eta_c \dot{\gamma} / \tau \qquad (2),$$

the ratio of hydrodynamic stress to shear stress (including all inter-particle interactions such as electrostatic, van der Waals, hydrolubrication, friction, and repulsive steric forces). The

viscosity of silicone oil in this study is η_c=10 mPa.s. Three *Mn** curves for the tests shown in Fig. 2 are plotted in Fig. 4a. The critical Mason numbers $Mn_c^* = \eta_c \dot{\gamma}_c / \tau_c$ for the onset of shear thickening (circular dots, τ_c is the critical shear stress) agree reasonably well with one another. ER fluids with different particle volume fractions (5-28%) and under different electric fields (0-5 kV/mm) also show similar $Mn_c^*=1.10\pm0.17\times10^{-6}$ for the onset of shear thickening, and $Mn_c^*=0.70\pm0.16\times10^{-6}$ for the onset of un-thickening, and E_c for the onset of shear thickening decreases from 4667 V/mm (4.3 %) to 533 V/mm (28 %). All these results indicate that the shear thickening of ER fluid occurs when *Mn** increases beyond about Mn_c^*, $E > E_c$, and $\dot{\gamma} \geq \dot{\gamma}_c$. Figure 4b shows voltage ramped tests under different constant shear rates. The Mn_c^* for shear thickening and un-thickening are about 1.3×10^{-6} and 0.8×10^{-6}, respectively (shown in Fig. 4c), consistent with the shear rate ramp tests shown in Fig. 2.

Figure 4b also shows that τ increases with *E* with different slopes *K*: K_1=1.1 Pa.mm/V is under the shear thickened state ($\tau = K \cdot E$, τ in Pa, *E* in V/mm). K_2 = 0.26 Pa.mm/V is under the un-shear thickened state, and decreases with increasing $\dot{\gamma}$ (under a higher $\dot{\gamma}$, where un-thickening can still happen, $K_2 \to 0$). The linear slopes of K_1 and K_2 are different from $\tau \propto E^2$ predicted by the traditional polarization models [8, 9, 14, 26]. Also, the linear variation of shear stress with *E* as shown in Fig. 4b is similar to the result reported in giant ER effect [6]. Due to the similar particle structures under the same shear rate, this linear relationship may indicate a linear relationship between the electrostatic interaction strength between particles in the *E* range of 600~2400 V/mm. It is different from the traditional polarization model and the conduction model predicted power of between one and two [8].

Equation 2 shows the importance of insulating liquid viscosity in the shear thickening of ER fluids. Therefore ER fluids with the same zeolite ER particles and the same particle volume fractions of about 24%, but different medium viscosities of 10, 50, 300, and 1000 mPa.s have been tested. The obtained Mn_c^* for the onset of shear thickening is about 10^{-4} for the ER fluids prepared with a 1000 mPa.s silicone oil, while is about 10^{-6} with 10 mPa.s silicone oil as shown in Fig. 5 (a). The later value agrees with results shown in Fig. 2-4. It indicates that Mn_c^* is not general for predicting the shear thickening of ER fluids. However, plotting the apparent viscosity of ER fluid versus shear rate, a critical apparent viscosity of ER fluids under electric fields for the shear thickening could be found as shown in Fig. 5(b). From Equation 2, the viscosity can be represented by the modified Mason's number as

$$\eta_{ST} = \tau / \dot{\gamma} = \eta_c / M_n^* \quad (3).$$

All the above experiments with a medium viscosity of 10 or 50 mPa.s, Mn_c^* obtained could give a reasonable agreement with the critical viscosity of ER fluids under electric fields. As shown in Fig. 5(c), the shear thickening happens at about η_{ST}= 0.8~2×10^4 Pa.s. However, the physical meaning of the critical bulk viscosity should be disclosed later.

3.3 An implication of shear thickening in ER fluids

For over 60 years, the shear yield stress of ER fluids has been mainly attributed to the attractive electrostatic interaction between particles [7-11,14-15,26] without experimental verification of the electrostatic interaction strength between ER particles. The ratio of shear stress change during shear thickening could be as high as 9, or even higher under higher

electric fields and particle volume fractions as found in our tests of various ER fluids not shown here. It could not be explained by the many-body effects considering the aggregation of particles from single chains to columns in ER fluids. The Madelung constant of a crystal structure of a cubic or body-centered tetragonal structure [14] is much less than 9. Also, the viscosity of colloidal suspensions could be increased by two orders of magnitude even with a particle interaction potential $U \to 0$ during shearing thickening [4, 5, 24, 25], which has been attributed to the direct or indirect mechanical contacts and the friction force of the contacts.

Therefore, if shear thickening is a general phenomenon in ER fluids, the friction force may play an important role in the origin of the shear resistance of ER fluids as sketched above in Fig. 1c. ER particles may be attracted or pushed together by the attractive electrostatic force F(r, θ) between particles and the shear thickening-induced load L to result in a friction force $F_f = f[F(r, \theta)+L]$, where f is the friction coefficient. The electric field E could increase the local particle concentration ϕ, induce an additional internal load $F(r, \theta)$, and a load L between the particles to facilitate the occurrence of shear thickening. E also controls the extent of shear thickening. Thus, the shear yield stress based on the friction force between particles could be controlled by the applied E. In fact, recently, the importance of friction force to the shear yield stress of ER and MR fluids prepared from fibers [29-31] and sea-urchin-like hierarchical morphology particles [32] has also been stressed by several research groups. For instance, column, zigzag, three-dimensional stochastic and near-planar stochastic structures of the magnetic fiber suspensions have been tested, the yield stress is found to mostly come from the restoring magnetic torque acting on each fiber and the solid friction between fibers [29-30].

3.4 Discussions with other experimental results

Considering the similarities between the ER effect and the MR effect, the friction force during shear thickening should also be directly responsible for the high shear yield stress of MR fluids. The friction force can explain why a normal compression of an ER/MR fluid can significantly increase the lateral shear yield stress of the ER/MR fluid by over one order of magnitude. This can also explain why the increase in yield stress is proportional to the applied pressure with a factor of about 0.3 [33], which is a typical value for the friction coefficient between two solid materials. The compression has a direct contribution to the load *L*. The shear yield stress τ_E of the ER fluid is related to the tensile yield stress σ_E through $\tau_E = 0.3\sigma_E$ [34]. Meanwhile, the shear thickening of a colloidal suspension consisting of smaller particles corresponds to a higher critical shear stress [2]. A similar inverse relationship between yield stress and particle diameter a of $\tau_s \propto 1/a$ has been obtained in a giant ER fluid [11]. Increasing the particle diameter from 20 nm to 1 μm, the yield stress of the giant ER fluid [11] under 5 kV/mm should decrease from 250 to 5 kPa, the same level of general ER fluids composed of micron-sized particles [14,15]. Therefore, the giant ER effect is essentially the same as the general ER effect. Both of them should be electric field-controlled shear thickening. The local electric field between particles in a giant ER fluid does not need to be over 100 k/mm as calculated in previous reports [10,16]. This electric field is far above the breakdown electric field strength of most insulating liquids. Decreasing particle size and increasing the friction coefficient between particles should be effective ways to increase the shear yield stress of both ER and MR fluids.

In the shear thickening of colloid suspensions, besides the parameters of particle volume fraction, particle size, particle shape and those of the host liquid [4], the particle interaction in the host liquid is also important [25, 35-37]. The jamming phase diagram for attractive particles shows that with a higher attractive strength, a lower particle volume fraction and a lower critical shear rate are required for the onset of jamming [25, 35]. Shear thickening would be suppressed by imposing a purely repulsive force field around each particle to prevent the particles to get close to each other [36]. The elasticity of suspensions formed by pre-shearing above the shear thickening transition could be scaled in a power law with the pre-shear stress [37]. The critical shear stresses for the same type of general colloidal suspension but with different particle volume fractions are the same [4-5]. In this study, the critical apparent viscosities for the shear thickening of ER fluids are similar as shown in Fig. 5b and 5c. When the dipolar interaction strength is not strong enough, or the applied electric field is not high enough, there is no shear thickening in ER fluids as shown in Fig. 2b.

The relationship between shear-thickening and yielding properties has also attracted much interest of researchers. In a recent report, people demonstrated that shear thickening of suspensions could be masked by a yield stress originating from particle interactions induced by applied electric field E or magnetic fields H, and confinement of hard particles at high packing fractions (ϕ). When E, H or ϕ are large enough, only shear thinning is observed [38]. This result agrees with shear thinning generally observed in ER/MR fluids at high shear rate and high E or H, shown by the main trend of curves in Fig. 5b. However, Fig. 5b also shows

local shear thickening around a low critical shear rate. We have also recently reported similar shear thickening phenomenon in MR fluids sheared between two parallel plates [39]. Thus, both geometries of concentric cylinders and two parallel plates could induce shear thickening of ER and MR fluids under high fields.

The shear thickening in ER fluids, a kind of dipolar suspension, has implications for the shearing of other dipolar suspensions. For instance, “frozen” water confined within a nanometer gap and under a high electric field [40] may also undergo a similar shear thickening process and behave like a solid. A thin polymer melt film confined between two smooth mica surfaces can also undergo such a similar shear thickening process [41]. The above results may predict clutch fluids with high friction forces triggered by applying a local electric field. Aside from electric/magnetic fields that could adjust particle interaction and induce shear thickening, other external stimuli such as light, heat, and electrochemistry may also be utilized to develop new field-responsive intelligent shear thickening materials.

4. Conclusions

Reversible electric field controlled shear thickening of ER fluids above certain low critical shear rate and high critical electric field strength has been reported in this study by shearing ER fluids between two concentric cylinders with various shearing modes. The onset of shear thickening and un-thickening could be well characterized by a critical apparent viscosity. While traditional polarization theory of ER effect generally ascribes the shear strength directly to the electrostatic attractive interaction strength between ER particles, the shear

thickening at very low shear rate indicates that friction force between particles originated from shear thickening may significantly contribute to the lateral shear resistance. The applied *E* can control the extent of shear thickening to change the shear resistance of ER fluids. This field controlled shear thickening in dipolar ER suspensions has implications for preparing advanced ER/MR fluids or ER/MR elastomers and the study of shearing other dipolar suspensions or liquids.

Acknowledgments

This work is supported by the National Natural Science Foundation of China (Grant No. 50875152) and the Program for New Century Excellent Talents in University of China. N.P., H.Z. and J.I. were supported by the U.S. Department of Energy, Office of Basic Sciences, Division of Materials Sciences and Engineering under Award # DE-FG02-87ER45331.

References

[1] Y. Komoda, T. N. Rao, A. Fujishima, Langmuir **13**, 1371 (1997).

[2] Y. J.Min, M. Akbulut, K. Kristiansen, Y. Golan , J. Israelachvili, Nature Materials **7**, 527 (2008).

[3] F. Caruso, R. A.Caruso, H. Mohwald, Science 282, 1111(1998).

[4] H. A. Barnes, J. Rheol. 33, 329 (1989).

[5] B. J. Maranzano, N. J. Wagner, J. Rheol. 45, 1205 (2001).

[6] M. J. Decker, C. J. Halbach, C. H. Nam, N. J. Wagner, E. D. Wetzel, Composites Sci. & Tech. 67, 565 (2007).

[7] W. M. Winslow, J. Appl. Phys. 21, 1137(1949).

[8] M. Parthasarathy, D. J. Klingenberg, Mater. Sci. & Eng. R: Reports 17, 57(1996).

[9] J. P. Coulter, K. D. Weiss, D. J. Calson, J. Intel. Mat. Sys. and Struc. 4, 248(1993).

[10] W.J. Wen, X. X. Huang, S. H. Yang, K. Q. Lu, P. Sheng, Nature Materials 2, 727(2003).

[11] W. J. Wen, X. X. Huang, P. Sheng, Appl. Phys. Lett. 85, 299 (2004).

[12] J. Rabinow, AIEE Trans. 67, 1308 (1948).

[13] J. M. Ginder, L. C. Davis, Appl. Phys. Lett. 65, 3410 (1994).

[14] D. J. Klingenberg, C. F. Zukoski, Langmuir 6, 15 (1990).

[15] Y. Tian, Y. G. Meng, S. Z. Wen, J. Appl. Phys. 90, 493 (2001).

[16] K.Q. Lu, R. Shen, X. Z. Wang, G. Sun, W. J. Wen, J. X. Liu, Chin. Phys. 15, 2476 (2006).

[17] J. E. Martin, J. Odinek, T. C. Halsey, Phys. Rev. Lett. 69, 1524 (1992).

[18] T.C. Halsey, W. Toor, Phys. Rev. Lett. 65, 2820 (1990).

[19] R. Tao, J. M. Sun, Phys. Rev. Lett. 67, 398 (1991).

[20] S. Henley, F. E. Filisko, J. Rheol. 43, 1323 (1999).

[21] E. M. Furst, A. P. Gast, Phys. Rev. E 62, 6916 (2000).

[22] K. von Pfeil, M. D. Graham, D. J. Klingenberg, Phys. Rev. Lett. 88, 188301 (2002).

[23] J.G. Cao, J. P. Huang, L.W. Zhou, J. Phys. Chem. B 110, 11635 (2006).

[24] C. J. O'Hern, S. A. Langer, A. J. Liu, S. R. Nagel, Phys. Rev. Lett. 86, 111 (2001).

[25] V. Trappe, V. Prasad, L. Cipelletti, P. N. Segre, D. A. Weitz, Nature 411, 772 (2001).

[26] C.W. Wu, H. Conrad, J. Phys. D 29, 3147 (1996).

[27] L.Y. Liu, X.X. Huang, C. Shen, Z. Y. Liu, J. Shi, W. J. Wen, P. Sheng, Appl. Phys. Lett. 87, 104106 (2005).

[28] Y. Tian, K. Q. Zhu, Y.G. Meng, S. Z. Wen, Int. J. Mod. Phys. B 19, 1311 (2005).

[29] P. Kuzhir, M.T. López-López, G. Bossis, J. Rheol. 53, 127 (2009).

[30] P. Kuzhir, M.T. López-López, G. Bossis, J. Rheol. 53, 115 (2009).

[31] M.T. López-López, P. Kuzhir, G. Bossis, P. Kuzhir, J.D.G. Duran, J. Mater. Chem. 17, 3839 (2007).

[32] J. B. Yin, X. P. Zhao, L. Q. Xiang, X. Xia, Z. S. Zhang, Soft Matter 5, 4687 (2009).

[33] X. Tang, X. Zhang, R. Tao, Int. J. Mod. Phys. B 15, 549 (2001).

[34] Y. Tian, , S. Z. Wen, H. R. Mao, Y. G.. Meng, Phys. Rev. E 65, 031507 (2002).

[35] J. Bergenholtz, J. F. Brady, M. Vicic, J. Fluid Mech. 456, 239 (2002).

[36] P. J. Lu, J. C. Conrad, H. M. Wyss, A. B. Schofield, and D. A. Weitz, Phys. Rev. Lett. 96, 028306 (2006).

[37] C. O. Osuji, C. J. Kim, D. A. Weits, Phys. Rev. E 77, 060402 (2008).

[38] E. Brown, N. A. Forman, C. S. Orellana, H. J. Zhang, B. Maynor, D. Betts, J. M. DeSimone, and H. M. Jaeger, Nature Mater. 9, 220 (2010).

[39] Y. Tian, J. L. Jiang, Y. G. Meng, S. Z. Wen, Appl. Phys. Lett. 97, 151904 (2010).

[40] E. M. Choi, Y. H. Yoon, S. Lee, H. Kang,. Phys. Rev. Lett. 95, 085701 (2005).

[41] G. Luengo, F. J. Schmitt, R. Hill, J. Israelachvili, Macromolecules 30, 2482 (1997).

Figures

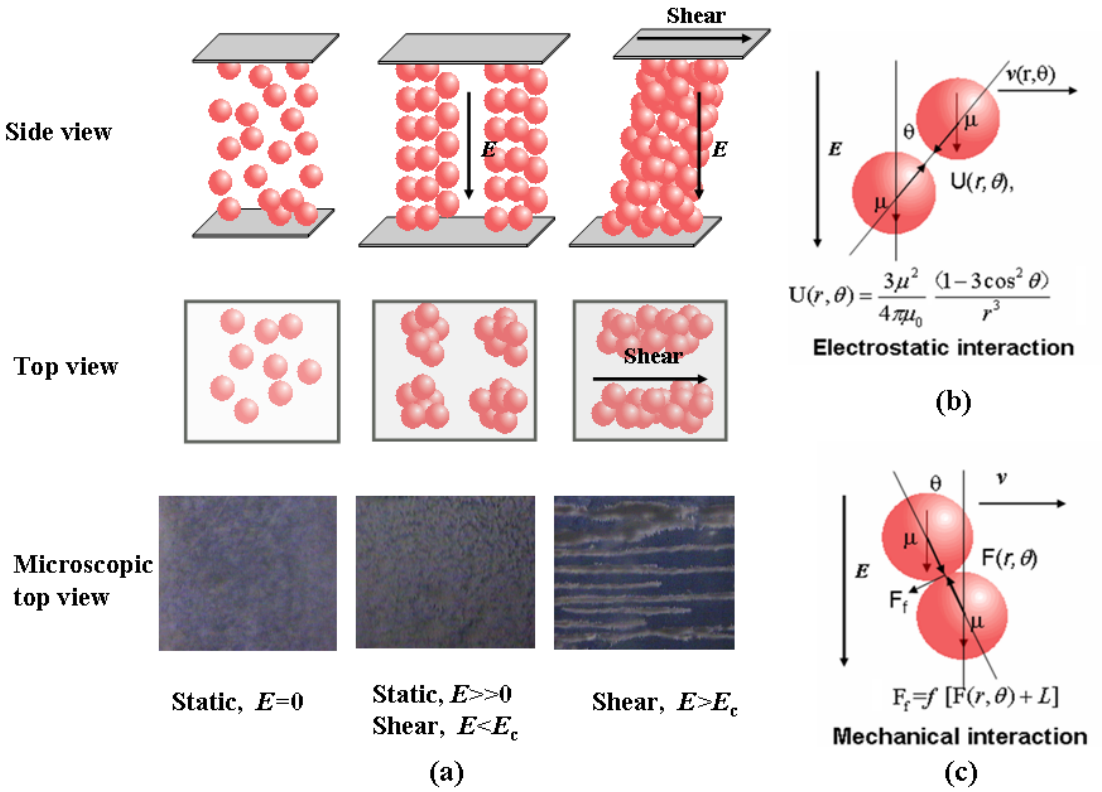

(Color online) Figure 1. Sketches of the ER effect and the origin of its shear resistance. (a) Side view, top view, and microscope top view of ER fluids under different electric fields E and shear states $\dot{\gamma}$. (b) Electrostatic pair interaction between particles in the traditional polarization model. (c) Mechanical interaction induced by the electrostatic interaction between particles after these particles become shear thickened or jammed.

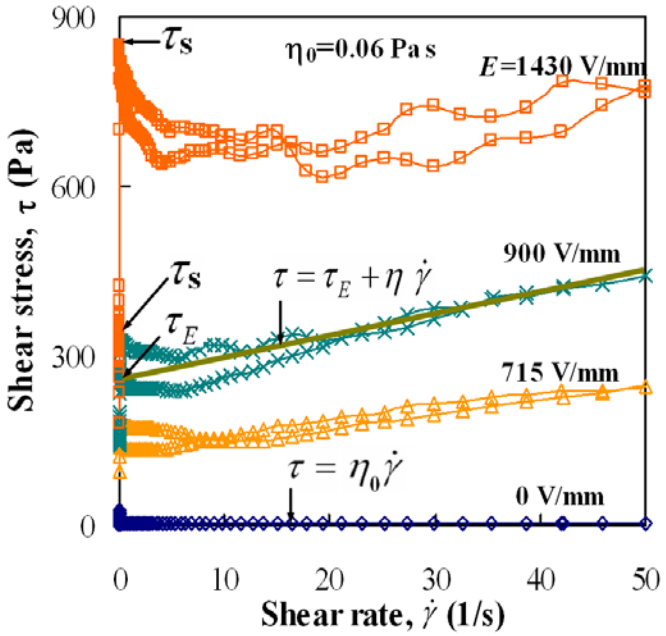
900
600
300
0
τ_S
η_0=0.06 Pa s
E=1430 V/mm
900 V/mm
τ_S
τ_E
$\tau = \tau_E + \eta\ \dot{\gamma}$
715 V/mm
$\tau = \eta_0 \dot{\gamma}$
0 V/mm
0
10
20
30
40
50
Shear stress, τ (Pa)
Shear rate, $\dot{\gamma}$ (1/s)

(a)

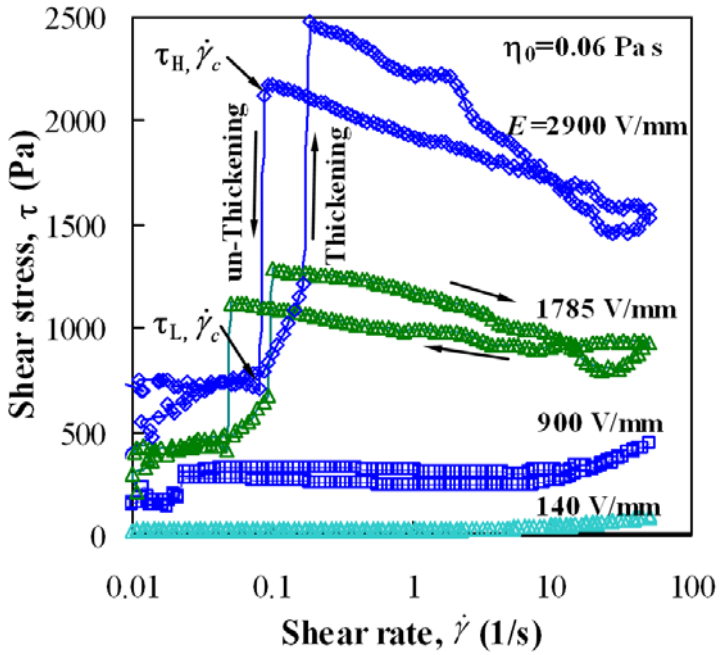
2500
2000
1500
1000
500
0
$\tau_{H,}\ \dot{\gamma}_c$
η_0=0.06 Pa s
E=2900 V/mm
un-Thickening
Thickening
1785 V/mm
$\tau_{L,}\ \dot{\gamma}_c$
900 V/mm
140 V/mm
0.01
0.1
1
10
100
Shear stress, τ (Pa)
Shear rate, $\dot{\gamma}$ (1/s)

(b)

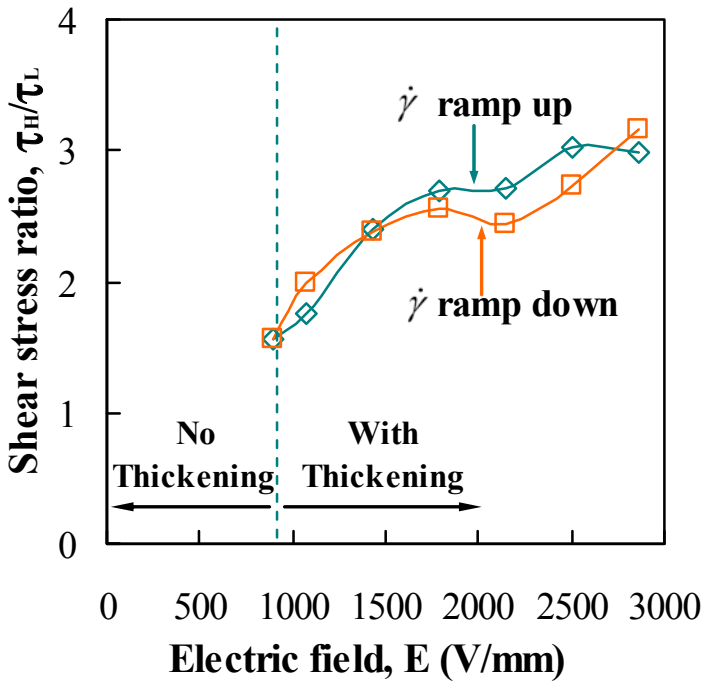

(c)

(Color online) Figure 2. Shear test results of an ER fluid with a particle volume fraction of 23% on a commercial rheometer (Physica MCR 301). (a) Shear curves of the ER fluid at different electric fields. (b) Shear curves with logarithmically plotted shear rates. (c) Ratio of high to low shear stress during shear rate ramp up and ramp down under different electric fields.

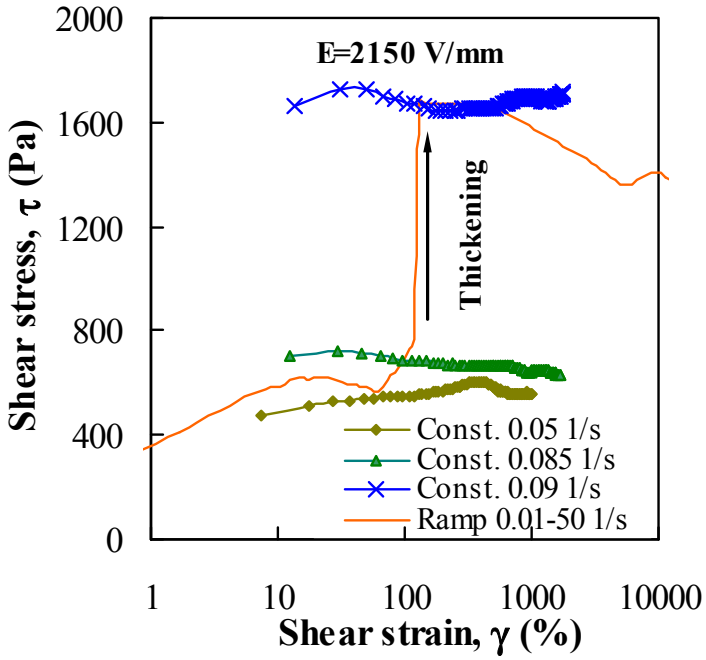
E=2150 V/mm
Thickening
Shear stress, τ (Pa)
Shear strain, γ (%)
Const. 0.05 1/s
Const. 0.085 1/s
Const. 0.09 1/s
Ramp 0.01-50 1/s
2000
1600
1200
800
400
0
1
10
100
1000
10000

(a)

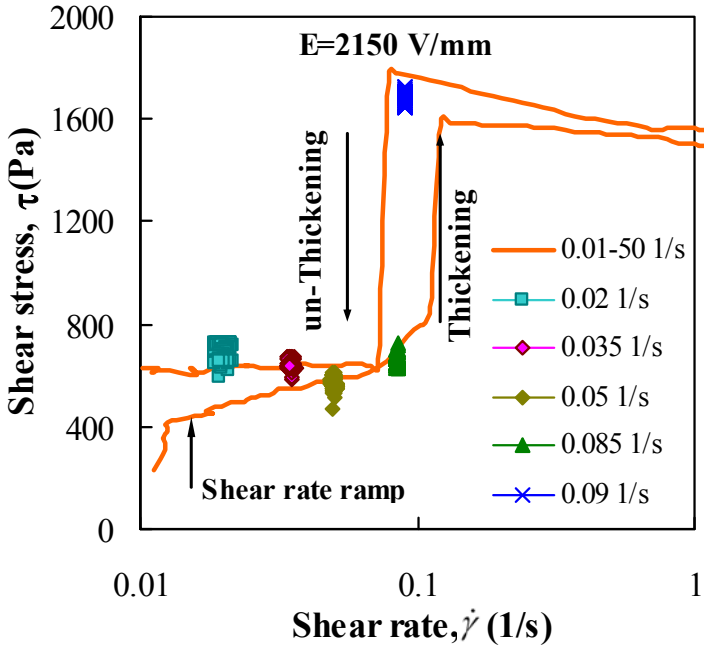
E=2150 V/mm
un-Thickening
Thickening
Shear rate ramp
Shear stress, τ(Pa)
Shear rate, $\dot{\gamma}$ (1/s)
0.01-50 1/s
0.02 1/s
0.035 1/s
0.05 1/s
0.085 1/s
0.09 1/s
2000
1600
1200
800
400
0
0.01
0.1
1

(b)

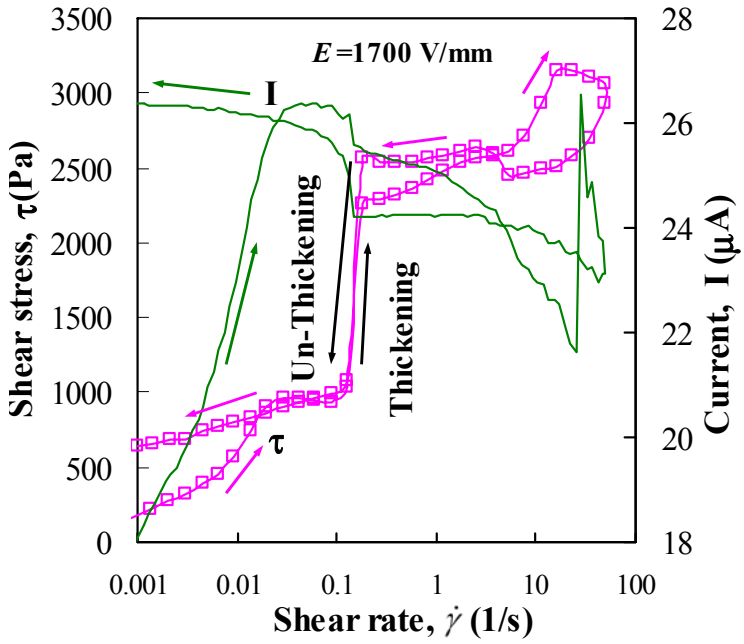

(c)

(Color online) Figure 3. Shearing at different constant shear rates and a current measurement. (a) Shear stress versus shear strain at different constant shear rates or shear rate ramp up under the same electric field of 2150 V/mm (particle volume fraction ϕ = 23%). (b) Shear stress versus shear rate at different constant shear rates or shear rate ramp up under the same electric field of 2150 V/mm (particle volume fraction ϕ = 23%). (c) Typical results of shear stress and current of the ER fluid (particle volume fraction ϕ = 28%) in a shear rate ramp test.

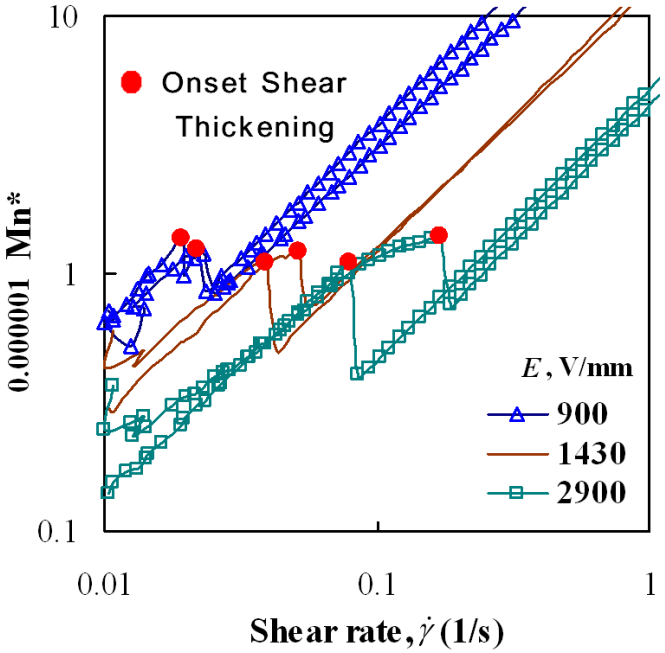
10
1
0.1
0.01
0.1
1
0.000001 Mn*
Onset Shear
Thickening
E, V/mm
900
1430
2900
Shear rate, γ̇ (1/s)

(a)

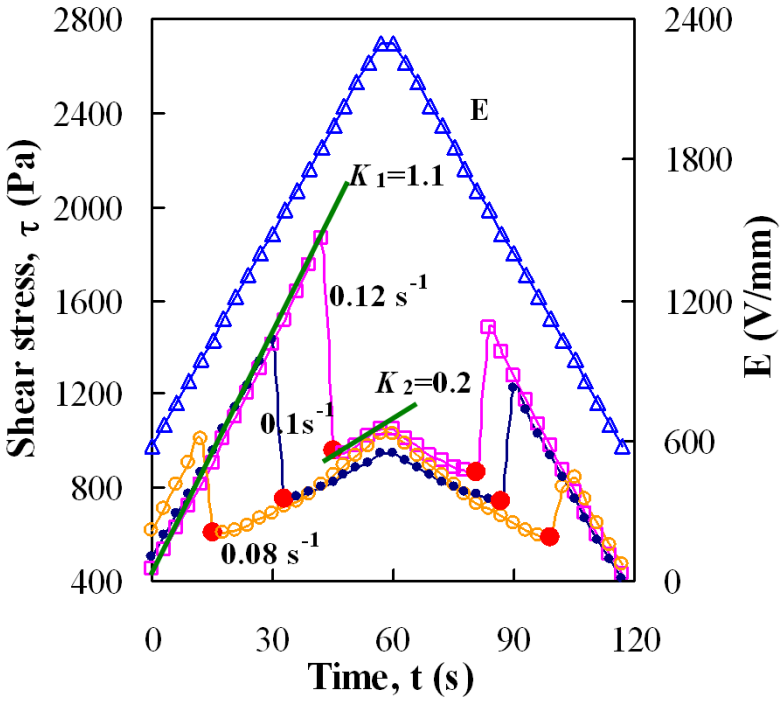
2800
2400
2000
1600
1200
800
400
2400
1800
1200
600
0
0
30
60
90
120
Shear stress, τ (Pa)
E (V/mm)
Time, t (s)
E
K 1=1.1
0.12 s-1
K 2=0.2
0.1s-1
0.08 s-1

(b)

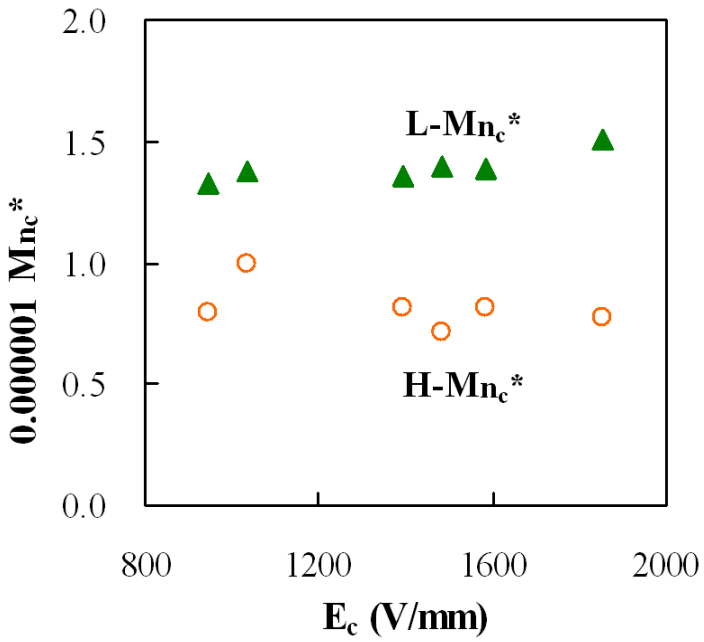

(c)

(Color online) Figure 4. The modified Mason number *Mn** in the shear thickening of ER fluids (particle volume fraction ϕ = 23%). (a) *Mn** curves of shear rate ramp tests replotted from Fig. 2. (b) Electric field ramp tests at a constant shear rate of 0.08, 0.1, or 0.12 s^{-1} with *E* ramped between 580 and 2300 V/mm. (c) Critical Mason numbers Mn_c* for the shear thickening shown in Fig. 4(b).

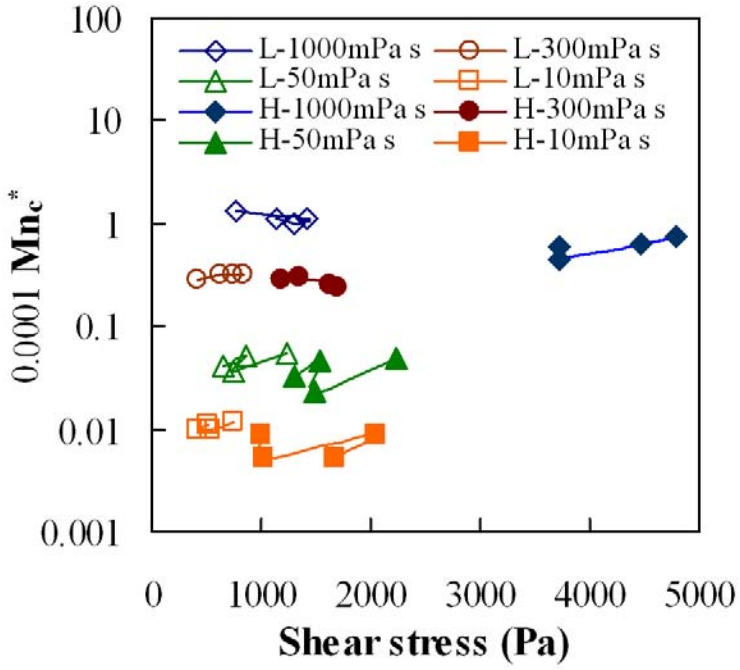
100
10
1
0.1
0.01
0.001
0.0001 Mnc*
L-1000mPa s
L-300mPa s
L-50mPa s
L-10mPa s
H-1000mPa s
H-300mPa s
H-50mPa s
H-10mPa s
0
1000
2000
3000
4000
5000
Shear stress (Pa)

(a)

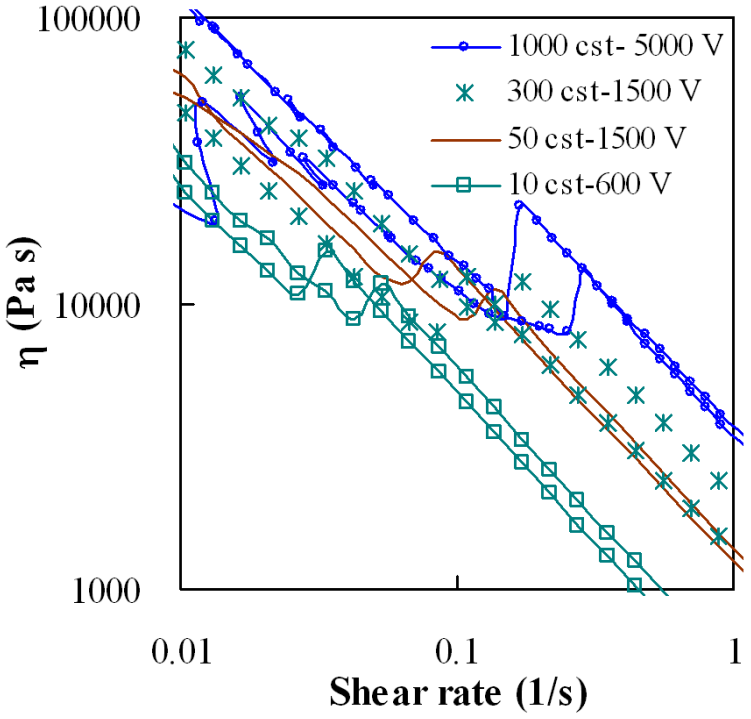
100000
10000
1000
η (Pa s)
1000 cst- 5000 V
300 cst-1500 V
50 cst-1500 V
10 cst-600 V
0.01
0.1
1
Shear rate (1/s)

（b）

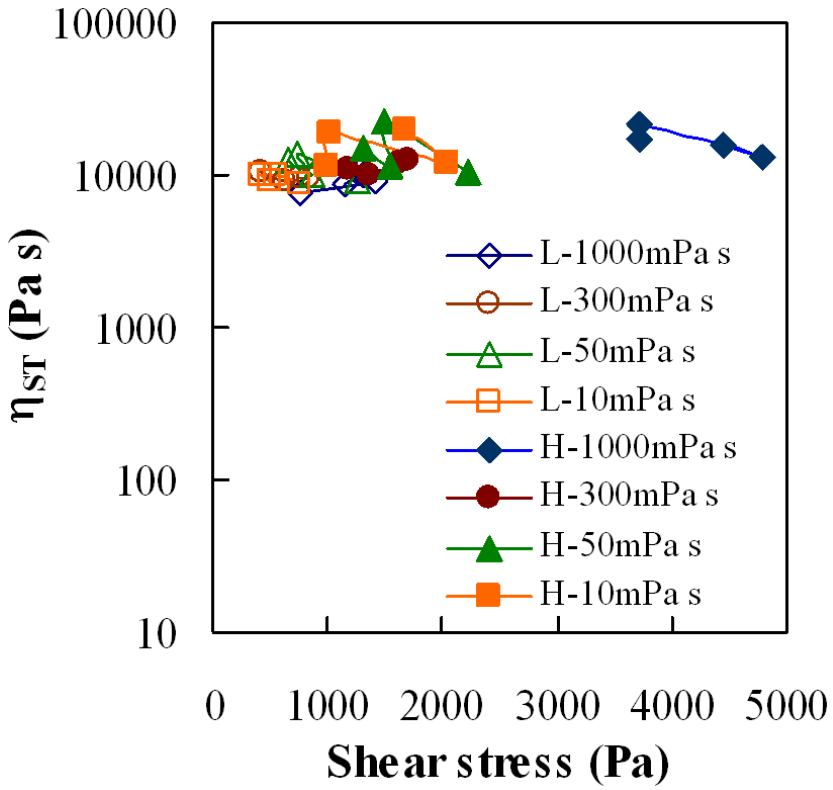

(c)

(Color online) Figure 5 Results of ER fluids with different silicone oil viscosities of 1000 mPa.s, 300 mPa.s, 50 mPa.s and 10 mPa.s, but with the same particle volume fraction of about 24%. (a) The critical Modified Mason numbers of ER fluids for shear thickening applied different electric fields, L means the low shear stress point before the shear stress jump, H means the high shear stress point after the shear stress jump; (b) Typical curves of the apparent viscosity of ER fluids during shearing; (c) The critical apparent viscosity of ER fluids for the shear thickening.